

## Target-Based Approach to Inhibitors of Histone Arginine Methyltransferases

Astrid Spannhoff,<sup>†</sup> Ralf Heinke,<sup>‡</sup> Ingo Bauer,<sup>§</sup> Patrick Trojer,<sup>||</sup> Eric Metzger,<sup>⊥</sup> Ronald Gust,<sup>#</sup> Roland Schüle,<sup>⊥</sup> Gerald Brosch,<sup>§</sup> Wolfgang Sippl,<sup>‡</sup> and Manfred Jung<sup>\*†</sup>

Institute of Pharmaceutical Sciences, Albert-Ludwigs-University of Freiburg, Freiburg, Germany, Institute of Pharmaceutical Chemistry, Martin-Luther University of Halle-Wittenberg, Halle, Germany, Division of Molecular Biology, Biocenter, Innsbruck Medical University, Innsbruck, Austria, Department of Biochemistry, Robert Wood Johnson Medical School, University of Medicine and Dentistry of New Jersey, Piscataway, New Jersey 08854, Centre for Clinical Studies, Albert-Ludwigs-University of Freiburg, Freiburg, Germany, and Institute of Pharmaceutical Chemistry, Freie Universität Berlin, Berlin, Germany

Received October 24, 2006

Lysine and arginine methyltransferases participate in the post-translational modification of histones and regulate key cellular functions. So far only one arginine methyltransferase inhibitor discovered by random screening was available. We present the first target-based approach to protein arginine methyltransferase (PRMT) inhibitors. Homology models of human and *Aspergillus nidulans* PRMT1 were generated from available X-ray structures of rat PRMTs. The NCI diversity set was filtered by a target-based virtual screening to identify PRMT inhibitors. Employing a fungal PRMT for screening and a human enzyme for validation, we have identified seven inhibitors of PRMTs in vitro. Hit validation was achieved for two new inhibitors by antibody mediated detection of histone hypomethylation as well as Western blotting in cancer cells. Functional activity was proven by an observed block of estrogen receptor activation. Thus, valuable chemical tools and potential drug candidates could be identified.

### Introduction

Histones are subject to a whole set of different post-translational modifications, such as acetylation and methylation, which together and depending on each other set a pattern of molecular signals for the access of transcription factors toward DNA, the so-called histone code.<sup>1–3</sup> The involvement of histone acetyltransferases and deacetylases (HDACs<sup>4</sup>) in central cellular functions such as apoptosis or differentiation has been studied in detail and their significance, for example, for the pathogenesis of malignant diseases, has been unravelled on a molecular level in several instances. Therefore, first clinical trials with HDAC inhibitors are currently under way.<sup>4,5</sup> Especially intriguing is the fact that certain nonhistone proteins are also acetylated and deacetylated.<sup>6–8</sup> Therefore, it is possible that reversible protein acetylation is a very general way for the regulation of the activity of certain proteins, and the same might be true for other modifications besides acetylation, such as methylation, as initial examples have been discovered.<sup>9,10</sup>

Detailed structure–activity relationships have been set up for HDAC inhibitors,<sup>3,5,11</sup> whereas much less is known in the area of histone methyltransferase inhibitors. Besides cofactor analogues like Sinefungin,<sup>11</sup> there is only one report each for inhibitors of lysine-<sup>12</sup> and arginine-<sup>13</sup>methyltransferases. In both cases, a random screening led to the discovery of new active compounds. The PRMT inhibitor AMI-1 (1; see Chart 1) shows

the potential to block transcriptional activation of androgen and estrogen receptors by agonists. An application to the treatment of hormone-dependent tumors with such inhibitors therefore seems feasible. Thus, rational approaches aimed at the identification of new PRMT inhibitors are interesting for both mechanistic studies as well as medicinal chemistry. We present the first successful results in that direction.

To identify inhibitors of PRMT, we applied a strategy that combined computational screening methods with a robust biochemical assay. A combination of molecular docking and pharmacophore-based filtering was used to conduct virtual screening with the National Cancer Institute (NCI) diversity set and a homology model of PRMT1. Compounds that were successfully docked by GOLD<sup>14</sup> and passed a simple structure-based pharmacophore were then selected and tested in a biochemical enzyme assay. Hit validation was achieved using antibody mediated detection of histone hypomethylation in cancer cells, and functional activity was observed for selected compounds in an estrogen receptor activation assay.

### Results and Discussion

**Virtual Screening.** As we have access to larger amounts of a recombinant PRMT1 homologue from *Aspergillus nidulans* termed RmtA,<sup>15</sup> we decided to use this enzyme as a screening tool. Up to now, no X-ray structure of a human or *A. nidulans* PRMT is available, but for the highly conserved rat PRMT1<sup>16</sup> and PRMT3<sup>17</sup> proteins structural data are available. However, the rat PRMT1 X-ray structures (pdb code 1OR8, 1ORI, 1ORH) are not suitable as target structures for virtual screening. The crystal structures of rat PRMT1 were obtained at an unphysiological pH value (pH 4.7; maximum enzymatic activity at pH 8.5). Additionally, an important helical section near to the binding pocket was not resolved in the PRMT1 X-ray structures (residues 1–40). An active and complete form of a rat PRMT is available only for the subtype 3 (pdb code 1F3L). Thus, we generated homology models for the active form of human PRMT1 and *A. nidulans* RmtA on the basis of the rat PRMT3 X-ray structure (for details, see the Experimental Section). The

\* To whom correspondence should be addressed: Prof. Dr. M. Jung, Institute of Pharmaceutical Sciences, University of Freiburg, Albertstraße 25, 79104 Freiburg, Germany. Tel.: +49-761-203-4896. Fax: +49-761-203-6321. E-mail: manfred.jung@pharmazie.uni-freiburg.de.

<sup>†</sup> Institute of Pharmaceutical Sciences, Albert-Ludwigs-University.

<sup>‡</sup> Institute of Pharmaceutical Chemistry, Martin-Luther University.

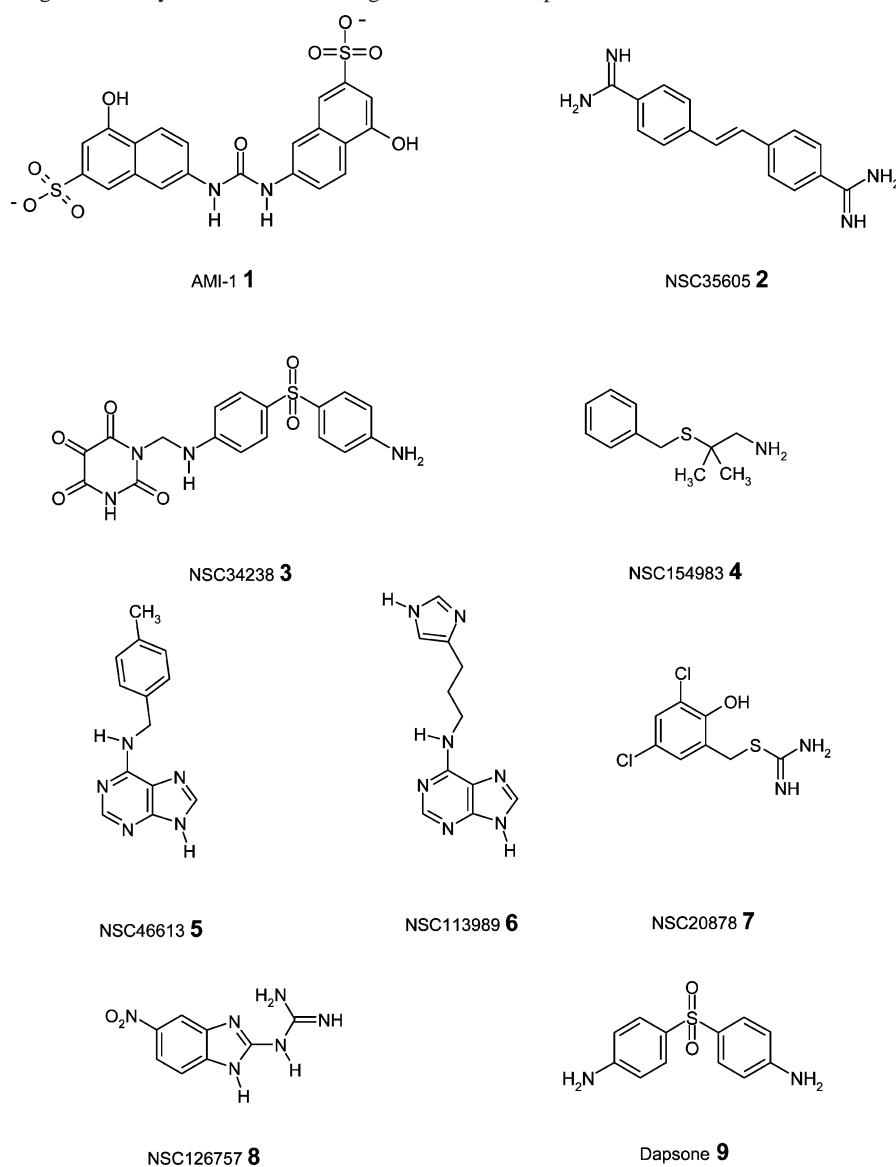
<sup>§</sup> Division of Molecular Biology, Innsbruck Medical University.

<sup>||</sup> Department of Biochemistry, University of Medicine and Dentistry of New Jersey.

<sup>#</sup> Centre for Clinical Studies, Albert-Ludwigs-University.

<sup>⊥</sup> Institute of Pharmaceutical Chemistry, Freie Universität Berlin.

<sup>a</sup> Abbreviations: HDAC, histone deacetylase; PRMT, protein arginine methyltransferase; NCI, National Cancer Institute; RmtA, arginine methyltransferase A; SAH, *S*-adenosyl homocysteine; SAM, *S*-adenosyl methionine.

**Chart 1.** Inhibitors of Arginine Methyltransferases and Negative Control Dapsone

sequence identity between the individual enzymes is sufficiently high for this approach, especially the residues within the binding pocket are highly conserved (human PRMT1 and PRMT3, 47% overall sequence identity; rat PRMT1 and *A. nidulans* RmtA, 59% identity; human PRMT1 and rat PRMT1, 95% identity; see sequence alignment in Supporting Information).

The PRMT X-ray structures and homology models were used for docking studies applying the program GOLD.<sup>14</sup> First, it was checked if GOLD was able to find the correct position of the cocrystallized ligands (cosubstrate analogue *S*-adenosylhomocysteine (SAH) cocrystallized with PRMT3 (1F3L) and with PRMT1 (1OR8) and the arginine side chain of the substrate cocrystallized with PRMT1 (1OR8)). GOLD was able to detect the position and conformation of both molecules within the 10 best docking poses for rat PRMT1 and PRMT3 with RMSD values below 1.5 Å (see Supporting Information). A similar orientation and conformation of SAH and arginine was obtained for the *A. nidulans* RmtA homology models due to the marginal differences between the enzymes of both species.

The generated *A. nidulans* RmtA homology model was subsequently used for virtual screening. The NCI diversity set, chosen as an initial database for lead compound identification, includes 1990 compounds derived from around 140 000 com-

pounds submitted to the NCI from a range of sources worldwide. In using this diverse subset of molecules as a compound source, we were able to screen a wide range of chemical structures for binding to PRMT1/RmtA using less extensive computational resources than would be needed to screen a more typically sized database. The use of different descriptors calculated with the program MOE<sup>18</sup> (see Experimental Section for details) excluded compounds that seemed to have undesirable pharmacokinetic properties. A total of 1630 compounds remained and were docked into the binding pocket using the *A. nidulans* RmtA model and the program GOLD (default docking adjustments). The substrate analogue SAH remained in the binding pocket and was regarded as a part of the protein during the docking.

In addition, using the *A. nidulans* RmtA homology model and the program GRID,<sup>19</sup> we calculated a detailed map showing favorable areas of interaction within the binding pocket (a positively charged amino probe and an aromatic carbon probe were used). Based on the GRID interaction fields, we calculated a simple pharmacophore model using the MOE PCH<sup>18</sup> pharmacophore generation tool. The derived pharmacophore, which consists of a cationic or hydrogen bond donor feature and two aromatic/hydrophobic features (Figure 1), was subsequently used to analyze the GOLD docking results. Only docking poses that

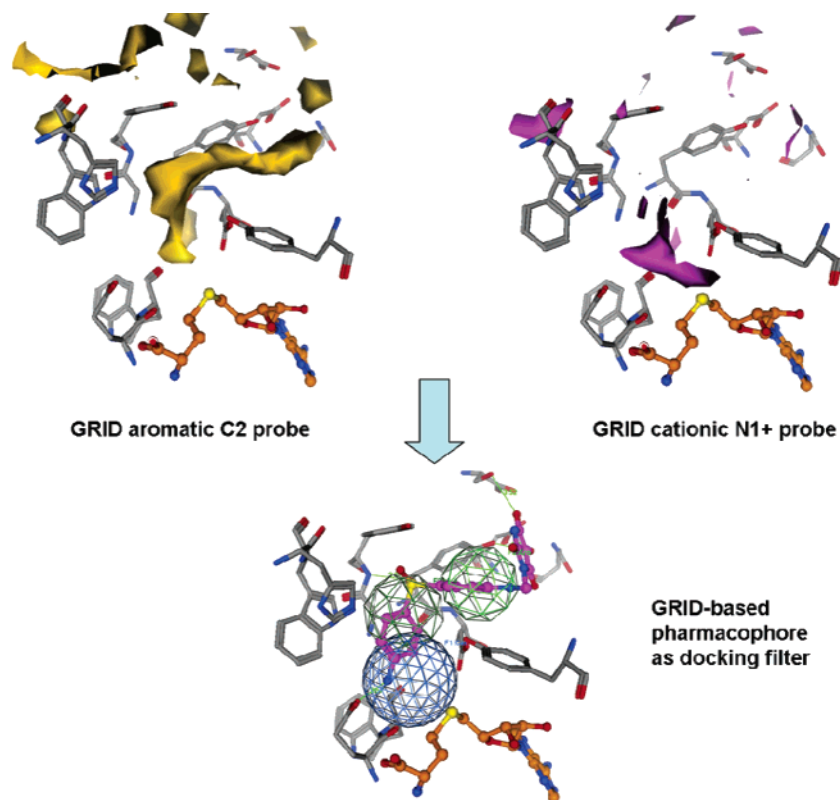


**Figure 1.** GRID-based pharmacophore. Based on the GRID interaction maps obtained with an aromatic (colored yellow) and a cationic nitrogen probe (colored purple), a simple pharmacophore was manually generated. Two aromatic/hydrophobic features (green spheres) and a cationic or hydrogen bond donor feature (blue sphere) were used. The pharmacophore model was applied as post-docking filter (exemplarily shown for compound **3**, colored magenta).

matched the pharmacophore were selected. The retrieved compounds were subsequently visually inspected based on the following criteria: (1) proximity of a polar/basic moiety of the ligand to Glu152 (numbering scheme of human PRMT1 is used) in the proposed binding mode; and (2) reasonable internal geometry of the inhibitor within the binding pocket. This analysis resulted in 36 compounds that were docked in addition to the human PRMT1 model. Similar orientations of the molecules within the binding pocket and comparable scores were obtained for the human enzyme. The selected 36 compounds were tested afterward in an in vitro assay for their ability to inhibit RmtA.

The interaction of two compounds **2** and **3** (see Chart 1) with human PRMT1 are shown as examples in Figures 2 and 3.

A common feature of the active inhibitors is the interaction (hydrogen bond) of a basic or polar group with the acidic residue Glu152. The basic moieties of the filtered compounds mimic the guanidine group of the arginine side chain of the substrate peptide. Compound **2** (Stilbamidine) makes additional hydrogen bonds with Asp336 and Ser353 located at the upper part of the binding pocket (Figure 2). The aromatic system interacts with the aromatic sidechains of Tyr156 and Tyr160 (not shown). The *trans*-stilbene aromatic system of stilbamidine is slightly rotated out of the plane, as are the amidines, with respect to the vicinal phenyl groups. However, the energy penalty between the docking solution and the planar conformation is below 10 kcal/mol (calculated with MMF94 and Tripos force field, as well as with AM1 semiempirical optimization). Compound **3** (that we call allantodapsonone) shows van der Waals interactions with several aromatic residues of the binding pocket (Tyr47, Tyr156, Trp302; and not shown, Tyr160) and accepts a hydrogen bond from the amide side chain of Asn333 (Figure 3).

Additionally, we compared the interaction mode of the detected hits with that of AMI-1 (**1**). For this purpose, **1** was docked into the *A. nidulans* RmtA and human PRMT1 protein model. Favorable docking poses could only be obtained when the cosubstrate SAH was omitted from the protein structure. Figure 4 shows the interaction mode of **1** in comparison with the cosubstrate derivative SAH in the human PRMT1 model. Both compounds show a similar type of interaction with the residues of the binding pocket. The sulfonyl groups of **1** make electrostatic and hydrogen bonding interactions with Lys40, Arg62, and Arg335, whereas the hydroxyl groups are involved in hydrogen bonds with Glu137 and the backbone carbonyl of Gly86 (not shown). The docking results (either for RmtA or human PRMT1) showed that **1** is likely to interact with the cosubstrate binding site rather than with the substrate pocket.

**Enzyme Inhibition Studies.** For the measurement of in vitro methyltransferase activity, we developed a new assay using a biotinylated oligopeptide that contains the amino acids 1–21 of histone H4 as the methylation substrate for *Aspergillus* RmtA. The peptide was immobilized on streptavidine-coated microtiter plates. Methylation was recognized using an antibody against dimethylR3 on H4. Treatment with an europium-labeled secondary antibody and final measurement of time-resolved fluorescence (TRF) was employed for the detection of the methylation level. A similar assay had been used previously for the detection of histone acetyltransferase activity on histones in cells.<sup>20</sup> In the course of our work, a related methyltransferase assay using a whole protein as the substrate and peroxidase-mediated chemiluminescence for the detection was published along with the discovery of **1**.<sup>13</sup>

Seven compounds showed a good inhibition in the europium assay and were then tested also with commercially available

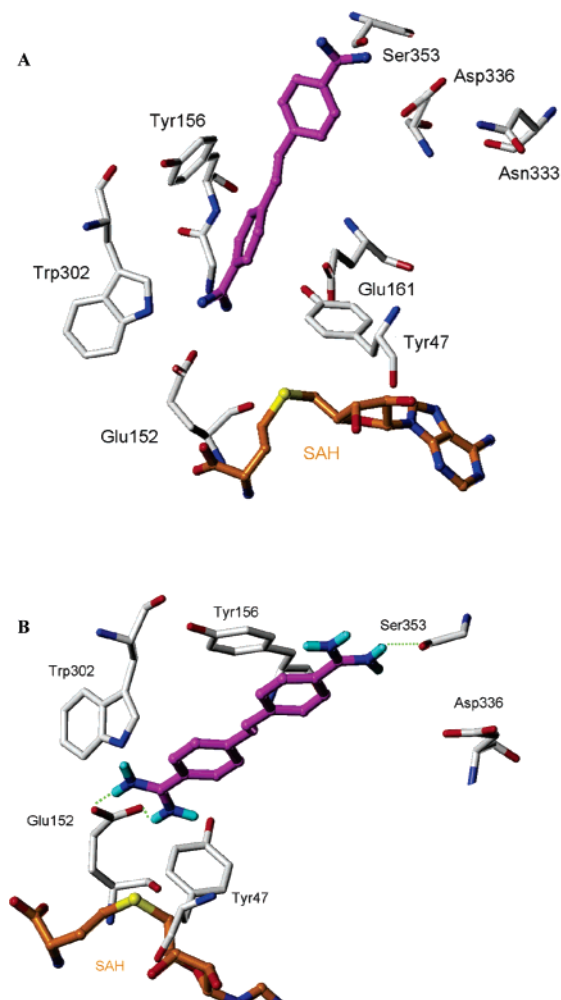


**Figure 2.** (A) Top ranked docking solution of **2** (magenta) into the human PRMT1 model (cosubstrate analogue SAH in orange). (B) Detailed view on the interaction of the polar amidine group, with residues at the entrance of the binding pocket. Hydrogen bonds between **2** and PRMT1 are displayed as dashed lines in green.

recombinant human PRMT1 (see Chart 1). Table 1 shows the  $IC_{50}$  values of the compounds for the fungal and the human enzyme. Inhibitor **1** was used as a reference (see Table 1). Based on the cellular data for two selected inhibitors, stilbamidine (**2**) and allantodapsone (**3**), kinetic analysis with the fungal enzyme and native core histones as substrates were performed. The data gives proof (see Figures 3 and 4 of Supporting Information) that both compounds are indeed competitive with regard to the protein substrate, as was intended by the virtual screening selection process and not for the cofactor SAM.

**Histone Hypomethylation.** For hit validation, the seven inhibitors were tested for their ability to induce histone hypomethylation caused by inhibition of PRMT1. We used a protocol with antibody-mediated detection of histone methylation after fixation of the cells.<sup>20</sup> As a negative control, we included the antilepra drug dapsone **9**, which is structurally related to **3** and does not inhibit RmtA in vitro. Only the reference compound **1** and the two new inhibitors **2** and **3** led to a dose-dependent inhibition of methylation on R3 in histone H4 (see Figure 5A). The detected methylation level was normalized to protein content. The determination of the protein content also showed that the compounds did not induce a pronounced antiproliferative effect in Hep G2 cells (data not shown). Compounds **4–8** did not show a significant hypomethylation (data not shown) and were not evaluated further.

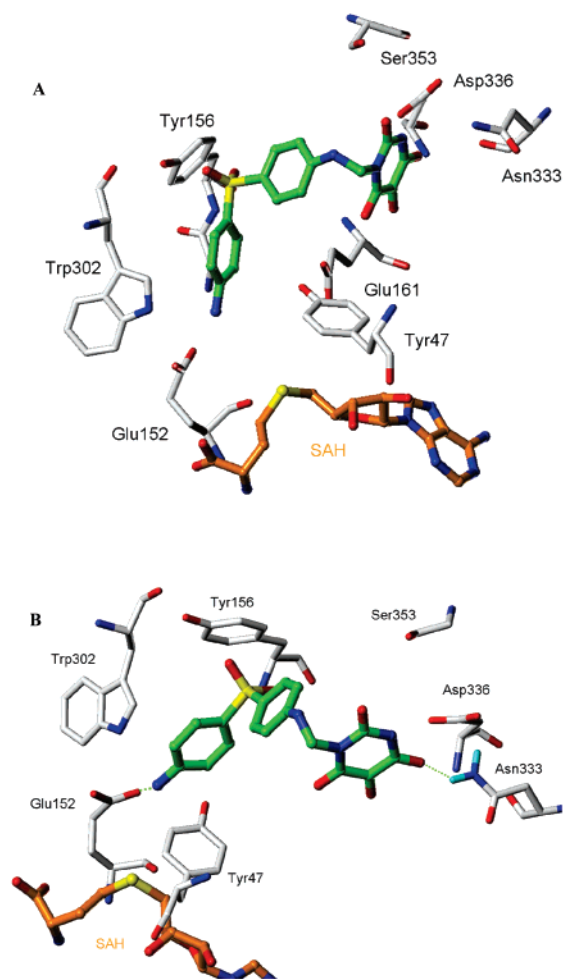


**Figure 3.** (A) Top ranked docking solution of **3** (green) in the human PRMT1 model (cosubstrate analogue SAH in orange). (B) Detailed view on the interaction of the polar allantoin group, with residues at the entrance of the binding pocket. Hydrogen bonds between **3** and PRMT1 are displayed as dashed lines in green.

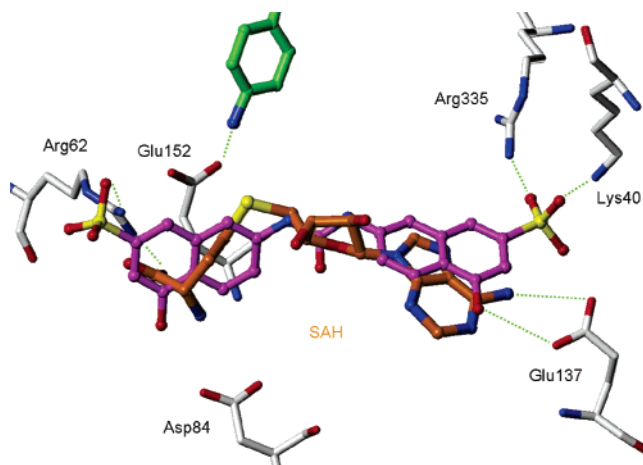


**Figure 4.** Top-ranked docking solution of **1** (magenta) within the cosubstrate binding pocket of the human PRMT1 model. The cocrystallized SAH (orange) and part of the docked inhibitor **3** (green) are shown for comparison.

Semiquantitative verification of histone hypomethylation was also performed by Western blot (see Supporting Information). Additionally, we investigated the inhibition of methylation on K4 by **1–3** in histone H3 (see Figure 5B). At 50  $\mu$ M, where more than 60% reduction of arginine methylation is observed for compounds **1–3**, only a slight reduction is observed for the

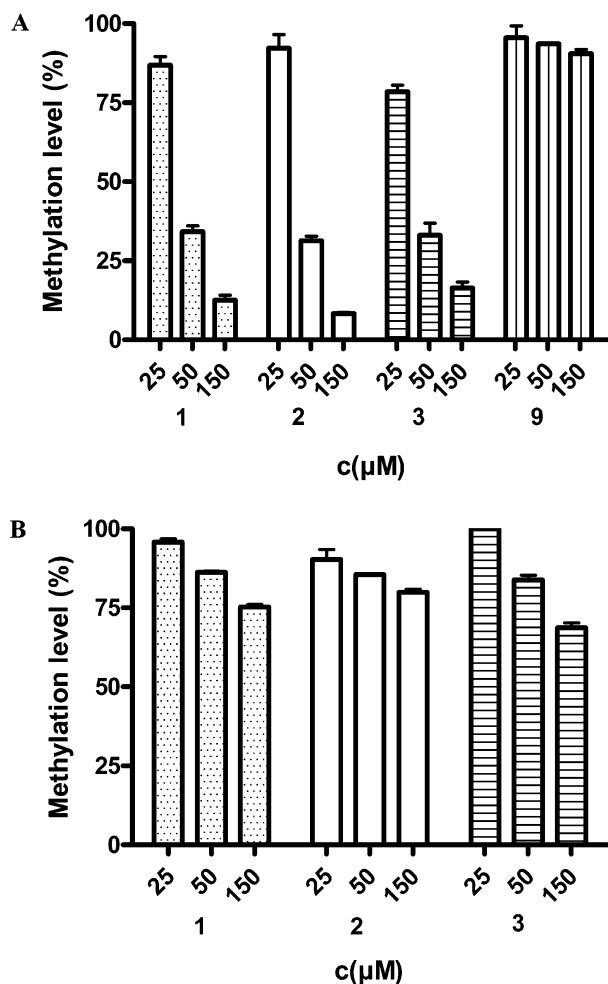


**Figure 5.** Bars reflect % methylation (100% = DMSO controls). Variation is <5% relative in all cases. (A) Signal (%) for methylation of H4R3. (B) Signal (%) for methylation of H3K4.

lysine methylation. At the maximum concentration, even for **1**, which has been reported to be selective for arginine over lysine methylation, a reduction up to 25% is monitored. Our compounds show a similar degree of selectivity.

**Transcriptional Activity.** The compounds that led to histone hypomethylation were then investigated in a functional assay. Arginine methyltransferases have been identified as coactivators for nuclear hormone receptors,<sup>21,22</sup> and the PRMT inhibitor **1** was shown to block activation of the androgen and the estrogen receptor in reporter gene assays. Measurements of the hormonal activity were performed using a MCF-7-2a cell line. This ER $\alpha$ -

**Table 1.** Inhibition of RmtA and hPRMT1

| cmpd | IC <sub>50</sub> ± SE (μM) or % inhibition, RmtA | IC <sub>50</sub> ± SE (μM), hPRMT1 |
|------|--|------------------------------------|
| 1    | 33.8 ± 7.8                                       | 1.2 ± 0.5                          |
| 2    | 29.9 ± 1.3                                       | 56.9 ± 6.2                         |
| 3    | 8.3 ± 0.3  | 1.7 ± 3.0                          |
| 4    | 68.3% at 10 μM                                   | 56.5 ± 4.6                         |
| 5    | no inhibition at 2 μM                            | 89.0 ± 4.6                         |
| 6    | 77.0% at 10 μM                                   | 54.8 ± 4.8                         |
| 7    | 26.1% at 2 μM                                    | 35.4 ± 3.4                         |
| 8    | 64.68% at 10 μM                                  | 76.1 ± 6.5                         |
|      | 34.9% at 2 μM                                    |                                    |
|      | 83.9% at 10 μM                                   |                                    |
|      | 18.3% at 2 μM                                    |                                    |
|      | 75.1% at 10 μM                                   |                                    |
|      | 15.6% at 2 μM                                    |                                    |

positive breast cancer cell line is controlled estrogen-dependent and stably transfected with the reporter plasmid ERE<sub>WT</sub>Luc. After receptor activation, luciferase activity is detectable, which is well correlated with the hormonal potency of test substances.<sup>23</sup> None of the tested inhibitors exhibited an estrogenic effect in concentrations up to 150 μM (data not shown). The incubation of cells with active compounds and 1 nM estradiol allows conclusions about antagonistic effects. Inhibitor **1** showed a moderate but significant inhibition of the receptor activation at a concentration of 150 μM (Figure 6) which correlates with its already published functional antagonism.<sup>13</sup>

Our new inhibitors showed high effects on receptor activation at this concentration. Stilbamidine (**2**) reduces the estradiol-induced luciferase activity by about 75%, whereas with Allantodapson (**3**), negative values were observed. This high antagonistic effect cannot be regarded independently from an existing cytotoxic effect in the MCF-7-2a cells. Antiproliferative effects as seen with potent antiestrogens reduce the cell number, resulting in negative values. The negative control dapsone did not show a block of receptor activation. So, for both positive and negative controls, a good correlation between the hypomethylation and the reporter gene assay was observed. Especially for **1** and **3**, much higher concentrations are required for cellular effects than for the *in vitro* inhibition. This could reflect binding to other PRMTs or generally other arginine binding factors but also simply poor cellular penetration or limiting stability. The high concentrations in the reporter gene model could also mean that the arginine methylation has to be blocked completely before an effect on transcription is observed. Improved inhibitors that are subject to ongoing work will serve to answer these questions.

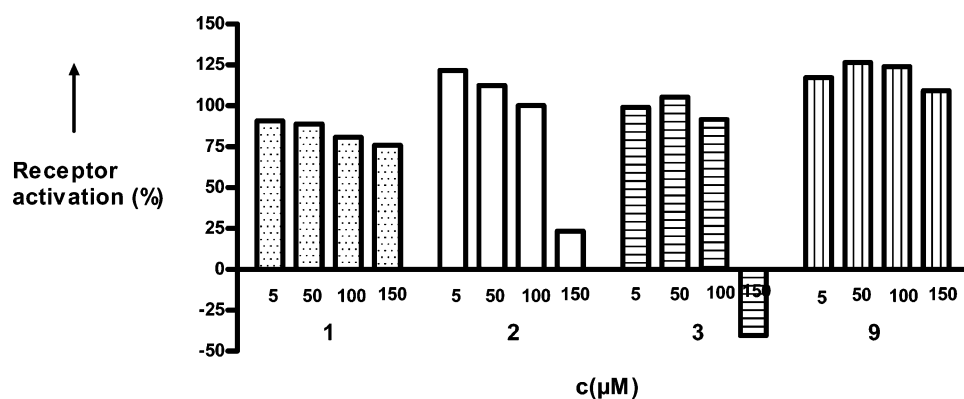


**Figure 6.** Inhibition of estradiol (E)-mediated receptor activation. For details, see ref 23. The compounds were coincubated in increasing concentrations with estradiol (1 nM). The extent of blocked estradiol induced luciferase activity is an indicator for the antagonistic effect.

## Conclusions

We successfully applied for the first time a structure-based approach toward the development of arginine methyltransferase inhibitors with cellular activity. In this field so far only one inhibitor had existed. This inhibitor **1** is due to its bisanionic structure most probably neither orally bioavailable nor would it penetrate the blood–brain barrier. Also, it resembles sulfonated ureas from the Suramin type, which have been reported to be pleiotropic drugs that target many proteins. Our new inhibitors lead to cellular hypomethylation and are active in a functional assay of estrogen receptor activation. Of course, further selectivity studies have to be performed, but due to their higher “drug-likeness”, they may now be used as lead structures for the study of structure–activity relationships and will serve as new tools for mechanistic investigations in the field of epigenetics. This in turn will be helpful to elucidate the therapeutic potential of this new class of potential drugs, especially in the treatment of hormone-dependent cancer.

## Experimental Section

**Inhibitors.** Inhibitor **1** was purchased from Chembridge and dapsone (**9**) was purchased from Sigma. The NCI diversity set, which represents a reduced set of 1990 compounds selected from the original NCI-3D structural database for their unique scaffolds, was obtained from the Office of the Associate Director, Developmental Therapeutics Program, Division of Cancer Treatment and Diagnosis, National Cancer Institute, U.S.A. More information is publicly available at [http://dtp.nci.nih.gov/branches/dscb/diversity\\_explanation.html](http://dtp.nci.nih.gov/branches/dscb/diversity_explanation.html).

**Molecular Modeling.** All calculations were performed on a Pentium IV 1.8 GHz based Linux cluster (16 CPUs). The 1990 compounds of the NCI diversity set were transformed into three-dimensional molecular structures using the MOE modeling package (Chemical Computing Group).<sup>18</sup> All compounds were generated in the protonation state that can be assumed under physiological condition. The use of different descriptors calculated with the program MOE<sup>18</sup> excluded compounds that seemed to have undesirable pharmacokinetic or physicochemical properties. The following limits were applied: molecular weight > 150 and < 500, topological surface area < 150 Å<sup>2</sup>, and logP < 7. In addition, compounds bearing metal ions were omitted from the data set. A total of 1630 compounds remained in the data set, which was used for the virtual screening.

**Protein Modeling.** The crystal structures of rat PRMT1 (pdb code 1ORI, 1ORH, 1OR8) and PRMT3 (pdb code 1F3L) were taken from the Protein Data Bank. The rat PRMT1 X-ray structures are not suitable as target structures for virtual screening. The crystal structures of rat PRMT1 were obtained at an unphysiological pH value (pH 4.7; maximum activity at pH 8.5) and an important helical section near to the binding pocket was not resolved in the PRMT1 X-ray structures. An active and complete form of a rat PRMT is available only for the subtype 3 (1F3L). A homology model for *A. nidulans* and human PRMT1 was generated using ClustalW sequence alignment of different PRMTs (see Supporting Information) and the COMPOSER module within Sybyl 7.1.<sup>24</sup> The rat PRMT3 (1F3L) X-ray structure was used as a template. The generated PRMT1 homology models were energy-minimized, applying a descent relaxation using the MMF94s force field and the GB/SA continuum solvent model for water within MOE. During the minimization, a tethering constant of 100 kcal/(mol Å) on the backbone atoms was applied, following a stepwise reduction of the tethering to 1 kcal/(mol Å).

**GRID Calculations.** Interaction possibilities were analyzed using the GRID program (Molecular Discovery Inc.). GRID is an approach to predict noncovalent interactions between a molecule of known three-dimensional structure (i.e., PRMT1) and a small group as a probe (representing chemical features of a ligand).<sup>19</sup> The calculations were performed using version 22 of the GRID

program and the PRMT1 homology models. The calculations were performed on a cube (20 × 20 × 20 Å, spacing 1 Å), including the adenine binding pocket, to search for binding sites complementary to the functional groups of the inhibitors. The following probes were used for calculation: positively charged amino probe (N1+) and aromatic probe (C2). Based on these two GRID fields, a simple pharmacophore was manually generated using MOE PHC features. The PRMT1 pharmacophore, which consists of a cationic or hydrogen bond donor feature (radius 2.6 Å) and two aromatic/hydrophobic features (radius 2 Å; Figure 1), was subsequently used to analyze the GOLD docking results. Only docking poses that match the pharmacophore were considered for further analysis.

**Docking.** The molecules of the NCI diversity set were docked at the putative binding site using the GOLD docking program (version 2.2) and default settings (Cambridge Crystallographic Data Centre).<sup>14</sup> Docking was carried out to obtain a population of possible conformations and orientations for these inhibitors at the putative active site. All torsion angles in each compound were allowed to rotate freely. Goldscore was chosen as the fitness function. For each inhibitor, docking runs were performed with a maximum allowed number of 10 poses. All docking solutions that passed the PRMT1 pharmacophore were stored in a MOE database for further analysis.

**Enzymes.** *Aspergillus* RmtA was expressed and purified as published.<sup>15</sup> For experimental details, also on human PRMT, see Supporting Information.

**In Vitro Time-Resolved Fluorescence Methyltransferase Assay.** The heterogeneous assay is performed in streptavidine-coated 96-well microplates (Nunc). After each incubation step, six wash steps are performed to remove the nonbound fraction. (Tecan Columbus plate washer; 300 μL/step in an overflow modus, performed with 100 mM Tris, containing 0.1% Tween 20; pH 7.5). First, the biotinylated substrate (aa 1–21 of human histone H4, Upstate, 20 pmol/well in 100 mM Tris, containing 0.1% Tween 20; pH 7.5) is bound to the cavities. In the second step, the bound substrate is turned over in an enzymatic reaction. Preincubation of the required amount of enzyme, 5 μL of inhibitor solution, and 10 μL of 15 mM Tris-buffer, pH 8.5, for 5 min at room temperature is recommended. Positive and negative controls are performed accordingly, but buffer instead of inhibitor is added. Then each mixture is transferred to its well and buffer is added to obtain a final volume of 200 μL. To start the enzyme reaction, 10 μL of an 800 μM SAM solution is added to all wells except for the negative control. The amount of the turnover is detected by a primary rabbit IgG antibody (anti-H4R3, Upstate, 200 μL of a 1:1000 dilution in 100 mM Tris containing 0.1% Tween 20 and 0.5% BSA, protease free; pH 7.5) and in a following step by a europium-labeled secondary antibody (Perkin-Elmer, 5 pmol/well, using the same buffer as for the first antibody reaction). The europium label is cleaved off by addition of an enhancement/chelating cocktail (Perkin-Elmer). After shaking the plate for 5 min with slow revolution, a final TRF measurement (340/615 nm, performed on a BMG Polarstar) is used for the quantitation.

**Histone Hypomethylation.** A total of 100 μL of Hep G2 cell suspension (100,000 cells/mL, 10,000 cells/well) is transferred to the wells of a 96-well microtiter cell culture plate (black, clear base CC3 plates, Nunc) and incubated for 24 h at 37 °C. An amount equal to 5 μL of compound dissolved in DMSO/phosphate buffered saline (PBS; equivalent to a final concentration of 0.16–0.99% DMSO) is added. The cells are incubated again for 72 h at 37 °C. Appropriate DMSO/PBS controls are included. The medium is tipped out and the cells are fixed and permeabilized by the addition of 100 μL of freshly prepared fixing solution containing 0.25% Triton-X 100, 0.25% glutardialdehyde, and 3.95% paraformaldehyde (all Fluka). The plate is incubated at 37 °C for 30 min. The wells are washed two times with PBS, and 100 μL of freshly prepared blocking solution (5% BSA) is added to each well. After incubation for 30 min at 37 °C, the wells are washed once with PBS. A total of 100 μL of primary antibody (anti-H4R3 rabbit IgG, Upstate) diluted 1/2000 in PBS is added to each well, and the plate is incubated for 1 h at 37 °C. The wells are washed once with 100

mM Tris, containing 0.1% Tween 20; pH 7.5. 100  $\mu$ L of a dilution of europium-labeled anti-rabbit IgG (Perkin-Elmer) (in 100 mM Tris containing 0.1% Tween 20 and 0.5% BSA, protease free, pH 7.5; dilution to 0.2  $\mu$ g/mL antibody concentration) is added to each well. The wells are washed once with 100 mM Tris, containing 0.1% Tween 20, pH 7.5. A total of 100  $\mu$ L of enhancement solution is added to each well, and fluorescence is measured in a time-resolved mode (340/615 nm). The wells are washed once with PBS, and protein concentration is estimated by the addition of 250  $\mu$ L of Bradford reagent (Sigma) to each well. The plate is shaken for 5 min with medium revolution and is then kept for 5 min at room temperature. Absorption is read at 600 nm. ELISA results are normalized by dividing the europium counts by protein measurement. The effect of inhibitors can then be compared with the DMSO-treated controls (0% reduction of methylation).

**Estrogen Receptor Reporter Gene Assays.** The experiments were performed as published.<sup>23</sup>

**Supporting Information Available:** Detailed procedures for cloning and purification of RmtA and PRMT1, radioactive methyltransferase assay using core histones, additional modeling figures and kinetic analysis showing the mode of inhibition for selected inhibitors **2** and **3** with native histones as substrates, and Western blot analyses for histone hypomethylation for **1–3**. This material is available free of charge via the Internet at <http://pubs.acs.org>.

## References

- Jenuwein, T.; Allis, C. D. Translating the histone code. *Science* **2001**, *293*, 1074–1080.
- Biel, M.; Wascholowski, V.; Giannis, A. Epigenetics—An epicenter of gene regulation: Histones and histone-modifying enzymes. *Angew. Chem., Int. Ed.* **2005**, *44*, 3186–3216.
- Schäfer, S.; Jung, M. Chromatin modifications as targets for new anticancer drugs. *Arch. Pharm. Chem. Life Sci.* **2005**, *338*, 347–357.
- Johnstone, R. W. Histone-deacetylase inhibitors: Novel drugs for the treatment of cancer. *Nat. Rev. Drug Discovery* **2002**, *1*, 287–299.
- Miller, T. A.; Witter, D. J.; Belvedere, S. Histone deacetylase inhibitors. *J. Med. Chem.* **2003**, *46*, 5097–5116.
- Gu, W.; Roeder, R. G. Activation of p53 sequence-specific DNA binding by acetylation of the p53 C-terminal domain. *Cell* **1997**, *90*, 595–606.
- Bereshchenko, O. R.; Gu, W.; Dalla-Favera, R. Acetylation inactivates the transcriptional repressor BCL6. *Nat. Genet.* **2002**, *32*, 606–613.
- Pagans, S.; Pedal, A.; North, B. J.; Kaehlcke, K.; Marshall, B. L.; et al. SIRT1 regulates HIV transcription via Tat deacetylation. *PLoS Biol.* **2005**, *3*, e41.
- Gu, H.; Park, S. H.; Park, G. H.; Lim, I. K.; Lee, H. W.; et al. Identification of highly methylated arginine residues in an endogenous 20-kDa polypeptide in cancer cells. *Life Sci.* **1999**, *65*, 737–745.
- Chuikov, S.; Kurash, J. K.; Wilson, J. R.; Xiao, B.; Justin, N.; et al. Regulation of p53 activity through lysine methylation. *Nature* **2004**, *432*, 353–360.
- Vedel, M.; Lawrence, F.; Robert-Gero, M.; Lederer, E. The antifungal antibiotic sinefungin as a very active inhibitor of methyltransferases and of the transformation of chick embryo fibroblasts by Rous sarcoma virus. *Biochem. Biophys. Res. Commun.* **1978**, *85*, 371–376.
- Greiner, D.; Bonaldi, T.; Eskeland, R.; Roemer, E.; Imhof, A. Identification of a specific inhibitor of the histone methyltransferase SU(VAR)3-9. *Nat. Chem. Biol.* **2005**, *1*, 143–145.
- Cheng, D.; Yadav, N.; King, R. W.; Swanson, M. S.; Weinstein, E. J.; et al. Small molecule regulators of protein arginine methyltransferases. *J. Biol. Chem.* **2004**, *279*, 23892–23899.
- Jones, G.; Willet, P.; Glen, R. C.; Leach, A. R.; Taylor, R. Development and validation of a genetic algorithm for flexible docking. *J. Mol. Biol.* **1997**, *267*, 727–748.
- Trojer, P.; Dangl, M.; Bauer, I.; Graessle, S.; Loidl, P.; et al. Histone methyltransferases in *Aspergillus nidulans*: Evidence for a novel enzyme with a unique substrate specificity. *Biochemistry* **2004**, *43*, 10834–10843.
- Zhang, X.; Cheng, X. Structure of the predominant protein arginine methyltransferase PRMT1 and analysis of its binding to substrate peptides. *Structure (London)* **2003**, *11*, 509–520.
- Zhang, X.; Zhou, L.; Cheng, X. Crystal structure of the conserved core of protein arginine methyltransferase PRMT3. *EMBO J.* **2000**, *19*, 3509–3519.
- Molecular Operating Environment (MOE)*; Chemical Computing Group Inc.: Montreal, Quebec, Canada, 2005.
- Goodford, P. J. A computational procedure for determining energetically favorable binding sites on biologically important macromolecules. *J. Med. Chem.* **1985**, *28*, 849–857.
- Wynne Aherne, G.; Rowlands, M. G.; Stimson, L.; Workman, P. Assays for the identification and evaluation of histone acetyltransferase inhibitors. *Methods* **2002**, *26*, 245–253.
- Chen, D.; Ma, H.; Hong, H.; Koh, S. S.; Huang, S. M.; et al. Regulation of transcription by a protein methyltransferase. *Science* **1999**, *284*, 2174–2177.
- Yadav, N.; Lee, J.; Kim, J.; Shen, J.; Hu, M. C.; et al. Specific protein methylation defects and gene expression perturbations in coactivator-associated arginine methyltransferase 1-deficient mice. *Proc. Natl. Acad. Sci. U.S.A.* **2003**, *100*, 6464–6468.
- von Rauch, M.; Busch, S.; Gust, R. Investigations on the effects of basic side chains on the hormonal profile of (4*R*,5*S*)/(4*S*,5*R*)-4,5-bis(4-hydroxyphenyl)-2-imidazolines. *J. Med. Chem.* **2005**, *48*, 466–474.
- SYBYL 7.0*; Tripos, Inc.: St. Louis, MO, 2005.

JM061250E